

## Lattice locations of silicon atoms in $\delta$ -doped layers in GaAs at high doping concentrations

R. C. Newman, M. J. Ashwin, M. R. Fahy, L. Hart, S. N. Holmes, C. Roberts, and X. Zhang  
*Interdisciplinary Research Centre for Semiconductor Materials, The Blackett Laboratory,  
 Imperial College of Science, Technology and Medicine, London SW7 2BZ, United Kingdom*

J. Wagner

*Fraunhofer-Institut für Angewandte Festkörperphysik, Tullastrasse 72, D-79108, Freiburg, Germany*  
 (Received 14 December 1995)

Low-noise infrared (IR) absorption measurements of localized vibrational modes (LVM's) showed that  $\text{Si}_{\text{As}}$  acceptors,  $\text{Si}_{\text{Ga}}\text{-Si}_{\text{As}}$  pairs, and a deep trap  $\text{Si-X}$  ( $V_{\text{Ga}}\text{-Si}_{\text{As}}\text{-As}_{\text{Ga}}$ ), as well as isolated  $\text{Si}_{\text{Ga}}$  donors, were present in silicon  $\delta$ -doping superlattices in (001) GaAs grown under an As flux by molecular-beam epitaxy (MBE) at 400 °C for areal concentrations (per layer)  $0.05 \text{ ML} \leq [\text{Si}]_A \leq 0.5 \text{ ML}$ . These observations supersede previous data, and agree with recent Raman-scattering measurements. For  $[\text{Si}]_A \geq 0.5 \text{ ML}$ , the LVM's were not detected by either technique, but Raman measurements revealed a broad line that has been attributed to small two-dimensional Si clusters. For  $[\text{Si}]_A \geq 0.5 \text{ ML}$ , electrical conductivity was lost. These observations led to a reappraisal of simulations of high-resolution x-ray 002 and 004 diffraction profiles. IR and Raman measurements for  $\delta$ -doping superlattices that all have  $[\text{Si}]_A = 0.01 \text{ ML}$  (per layer) showed only the  $\text{Si}_{\text{Ga}}$  LVM as the interlayer spacing was reduced to 5 ML when the volume carrier concentration  $n$  approached  $\sim 2 \times 10^{19} \text{ cm}^{-3}$ . For interlayer spacings of 2 and 1 ML, compensating complexes  $\text{Si}_{\text{As}}$ ,  $\text{Si}_{\text{Ga}}\text{-Si}_{\text{As}}$ , and  $\text{Si-X}$  were present, and  $n$  tended to zero. Compensating complexes were also present in homogeneously doped MBE GaAs grown at 350 °C, but  $n$  remained at a value of  $2 \times 10^{19} \text{ cm}^{-3}$  as  $[\text{Si}]$  was increased to  $1.3 \times 10^{20} \text{ cm}^{-3}$ .  $n$  never exceeded  $2 \times 10^{19} \text{ cm}^{-3}$  in any sample. The formation of  $V_{\text{Ga}}$ ,  $\text{As}_{\text{Ga}}$ , etc. is attributed to diffusion jumps of Si atoms originally located on Ga lattice sites. The formation of the "Si-like" structure in  $\delta$  layers must result from the aggregation of such displaced atoms. We speculate that these processes are facilitated by the initial displacements of  $\text{Si}_{\text{Ga}}$  donors to  $DX$  locations. [S0163-1829(96)01536-6]

### I. INTRODUCTION

Silicon  $\delta$  doping of GaAs grown by molecular-beam epitaxy (MBE) is an alternative to homogeneous  $n$ -type doping, and is useful for the fabrication of certain types of device.<sup>1,2</sup> The growth procedure is to interrupt the Ga flux, deposit the required areal concentration of Si atoms  $[\text{Si}]_A$  (per layer), and then to reinstate the Ga flux to obtain an overgrowth of GaAs. This sequence may be carried out many times at regular intervals to produce a  $\delta$ -doping superlattice. During the Si deposition, the As flux may be either continued<sup>3</sup> or shuttered.<sup>4</sup> In the present work only the former method is employed. An ideal structure resulting from the deposition of a single  $\delta$  layer would consist of a sheet of ionized Si atoms all occupying Ga-lattice sites ( $\text{Si}_{\text{Ga}}$ ) in a single atomic plane with the electrons occupying states in subbands in the adjacent  $V$ -shaped potential well.<sup>5,6</sup> The real situation is more complicated, and there have been problems in understanding the evolution of the atomic structure of layers, as  $[\text{Si}]_A$  is increased to a value equal to or greater than  $\sim 3.1 \times 10^{14} \text{ cm}^{-2}$ , corresponding to 0.5 ML of Si. This concentration would correspond to the substitution of all the Ga atoms by Si atoms in a single atomic layer. The numerical distinction between  $3.1 \times 10^{14} \text{ cm}^{-2}$  and a higher value  $3.4 \times 10^{14} \text{ cm}^{-2}$ , to allow for the smaller lattice spacing of Si, is insignificant in this work.

MBE growth on a (001) GaAs surface is usually carried out at a temperature  $T_g \sim 580$  °C. Because of surface segregation, Si impurity atoms are distributed throughout a layer

with a thickness of more than 20 ML above the  $\delta$  plane on which they are deposited. Surface segregation has been demonstrated directly by secondary-ion-mass spectrometry (SIMS) measurements<sup>6-8</sup> and by Raman measurements of the depth dependence of the scattering from localized vibrational modes (LVM's) of the Si atoms present in the overgrowth.<sup>9,10</sup> A similar distribution was inferred from *in situ* reflection high-energy electron-diffraction (RHEED) observations<sup>11</sup> that reveal progressive changes in the (001) GaAs surface from a  $3 \times 1$  reconstruction, via an asymmetric  $3 \times 1$  reconstruction to a  $2 \times 4$  reconstruction as the  $\delta$  layer is overgrown. An extrapolation of published SIMS measurements<sup>6,7</sup> indicates that the segregation process should be effectively eliminated if  $T_g$  is lowered to 400 °C: this is the growth temperature used in our previous<sup>3</sup> and present studies of Si  $\delta$ -doping superlattices. Analysis of high-resolution x-ray measurements of the 004 and 002 reflections and the associated satellite structure arising from stacks of 60 or 100 nominally equally spaced  $\delta$  layers with  $[\text{Si}]_A = 0.5 \text{ ML}$  (Ref. 12) showed that the spreading of the Si atoms was no greater than 2.0 ML (5.6 Å) (the resolution limit), confirming that surface segregation was indeed inhibited.

Recent Raman data<sup>13</sup> showed that as  $[\text{Si}]_A$  was increased (for single  $\delta$  layers), the strength of the scattering from the LVM due to isolated  $\text{Si}_{\text{Ga}}$  donors increased initially, but then passed through a plateau and eventually fell, so that the line was undetectable for a Si coverage of  $\sim 0.5 \text{ ML}$ . In addition, lines from  $\text{Si-X}$  (a deep electron trap, argued to be a planar

As<sub>Ga</sub>-Si<sub>As</sub>-V<sub>Ga</sub> defect<sup>14</sup>), and Si<sub>Ga</sub>-Si<sub>As</sub> donor-acceptor pairs were observed for  $[\text{Si}]_A \geq 0.1$  ML (see Fig. 2 in Ref. 13): the strengths of these lines also increased, only to decrease to zero again when  $[\text{Si}]_A$  reached 0.5 ML. At the stage when these Si LVM's became undetectable, a broad scattering feature (line A) appeared at a frequency in the range 470–490 cm<sup>-1</sup>. This line has been attributed to the vibrational mode(s) of covalently bonded Si atoms, present in the form of small clusters that constitute a  $\delta$  phase, distinct from isolated Si<sub>Ga</sub>-Si<sub>As</sub> donor-acceptor pair defects found in heavily homogeneously doped GaAs. Previous simultaneous observations<sup>4</sup> of line A and LVM's due to Si occupying Ga or As lattice sites in the GaAs matrix in the spectra of samples with  $[\text{Si}]_A = 0.7$  ML grown at  $T_g = 580$  °C do not constitute a discrepancy with these later results. The difference is explained by surface segregation of the Si atoms and the diffusion of Si atoms out of the  $\delta$  phase,<sup>15</sup> because of the higher growth temperature.

Earlier IR-absorption measurements<sup>3</sup> made on  $\delta$ -doping superlattices showed that the strength of the Si<sub>Ga</sub> LVM exhibited the same dependence on  $[\text{Si}]_A$  as that found by Raman scattering, but lines due to Si<sub>As</sub>, Si<sub>Ga</sub>-Si<sub>As</sub> pairs, Si-X complexes, and line A were not detected for any value of  $[\text{Si}]_A$ . The presence of a steeply sloping background due to free-carrier absorption made it difficult to detect weak LVM lines. It was pointed out that the LVM from Si<sub>Ga</sub> is narrower than the lines from Si<sub>As</sub>, Si<sub>Ga</sub>-Si<sub>As</sub> pairs, and Si-X, and the detection limit for Si<sub>As</sub>, was estimated to be a factor of 3 times greater than that for Si<sub>Ga</sub>: the detection limit for Si-X would be even higher. Line A may have a small dipole moment so that it is effectively IR inactive, but the discrepancy with respect to the observations of the LVM's from Si<sub>As</sub> and Si<sub>Ga</sub>-Si<sub>As</sub> is significant. Consequently, additional IR measurements have been made on  $\delta$ -doping superlattices using a Bruker IFS 120HR interferometer rather than the IFS 113v model used previously, enabling spectra to be obtained with a better signal-to-noise ratio. In addition, improved procedures have been used for the subtraction of the free-carrier background and intrinsic two-phonon absorption from GaAs, allowing LVM lines to be more easily revealed. Briefly, we shall demonstrate that LVM lines due to Si<sub>As</sub>, Si<sub>Ga</sub>-Si<sub>As</sub> pairs, and Si-X are present in the IR spectra of  $\delta$ -doping superlattices with  $0.05 \leq [\text{Si}]_A \leq 0.5$  ML, leading to a general consistency with the Raman measurements.

The carrier concentrations  $n$  of  $\delta$ -doping superlattices (grown at 400 °C) increased initially as  $[\text{Si}]_A$  was increased, but followed the trend in the strength of the Si<sub>Ga</sub> LVM by reaching a maximum value  $n_{\text{MAX}}$  before falling to a value close to zero when  $[\text{Si}]_A$  reached 0.5 ML.<sup>3</sup> Knowledge about spreading due to segregation and diffusion processes is clearly important to the interpretation of electrical measurements, where conduction of doped GaAs adjacent to the  $\delta$  phase has to be distinguished from that of the  $\delta$  phase itself. Possible reasons for the loss of conductivity have been discussed in relation to the loss of isolated Si<sub>Ga</sub> donors.<sup>16,17</sup> Comparisons with the IR absorption and Raman LVM scattering of  $\delta$  layers incorporating isoelectronic Al<sub>Ga</sub> (Ref. 18) led to the conclusion that at some stage in the growth of Si  $\delta$  layers, there were changes in the lattice sites and/or the charge states of deposited Si<sub>Ga</sub> atoms as  $[\text{Si}]_A$  was increased

toward 0.5 ML. There was a suggestion that local rafts of alternate Si<sub>Ga</sub><sup>+</sup> donors and Si<sup>-</sup> (DX centers<sup>19</sup>) formed, leading to displacements of up to 50% of the Si<sub>Ga</sub> atoms from their tetrahedral sites.<sup>3,17</sup> The assignment of line A in Raman spectra (see Fig. 2 in Ref. 13) to planar clusters of covalently bonded Si would additionally imply a transfer of 50% of the Si atoms from Ga sites to As-sites to form (Si<sub>Ga</sub>-Si<sub>As</sub>)<sub>n</sub> structures, unless Si atoms were displaced into interstitial sites and then diffused to form clusters. A possibility that a compound structure Si<sub>3</sub>As<sub>4</sub> was generated<sup>17</sup> was also considered, because of the presence of excess As during the deposition of the Si.

Scanning tunneling microscopy (STM) (Ref. 20) has been used to study the deposition of Si atoms on to a GaAs c(4×4)-reconstructed (001) surface held at 400 °C. An important observation was that of Si-atom clustering to produce streamers along the [110] direction due to surface diffusion once  $[\text{Si}]_A$  exceeded  $\approx 0.1$  ML (when anisotropy was first observed): clustering was, however, detected for Si coverages as low as  $[\text{Si}]_A = 0.02$  ML.<sup>21</sup> Such clusters, buried by an overgrowth of GaAs, help to lead to an explanation of line A observed in Raman spectra from samples containing  $\delta$  layers with larger values of  $[\text{Si}]_A$ . The STM results were explained by models for which all the Si atoms occupied Ga-surface sites for coverages  $[\text{Si}]_A$  up to 0.5 ML. The validity of the models is still unclear, but the proposed interpretation is not excluded by the IR and Raman data, since it has been inferred previously that diffusion jumps of Si atoms occur leading to local site switching during the subsequent overgrowth of the surface with GaAs.<sup>17,22</sup>

IR and Raman measurements have also been made on  $\delta$ -doping superlattices<sup>23</sup> with  $[\text{Si}]_A = 6 \times 10^{12}$  cm<sup>-2</sup> (0.01 ML), when the Si atoms continue to occupy predominantly Ga lattice sites after the GaAs overgrowth, and there is corresponding  $n$ -type conductivity, provided the layers are widely separated (560 Å or  $\sim 200$  ML).<sup>3</sup> The effect of reducing the interplanar spacing from 200 to 1 ML was then investigated (see also Ref. 24). These measurements are complemented by similar studies made on homogeneously doped samples grown at 350 °C. Briefly, none of these samples showed detectable Raman scattering from the complexes giving rise to line A, and so there was no evidence of long-range diffusion of Si atoms. There was, however, evidence that not all Si atoms occupied substitutional sites in the GaAs matrix. The latter result is significant in understanding the processes that limit the maximum volume concentration of carriers to  $n_{\text{MAX}} \sim 2 \times 10^{19}$  cm<sup>-3</sup>, and in this context they link to the measurements made on the samples containing highly doped  $\delta$  layers.

Since covalently bonded planar Si clusters appear to be the predominant species present in  $\delta$  layers when  $[\text{Si}]_A \geq 0.5$  ML, and the full range of Si centers is present for somewhat smaller areal concentrations, it is necessary to reconsider the modeling of our previous x-ray measurements.<sup>12</sup> Various structures were shown to be consistent with the measurements, although in the most recent studies<sup>15</sup> emphasis was given to structures incorporating primarily Si<sub>Ga</sub> atoms because in our earlier work only Si<sub>Ga</sub> donors had been detected in IR LVM spectra. To carry out simulations, it is necessary to specify the bond lengths for Si<sub>Ga</sub>-As, Si<sub>As</sub>-Ga, and Si<sub>Ga</sub>-Si<sub>As</sub>. Previously, we obtained bond lengths from

TABLE I. Details of  $\delta$  superlattices with various values of  $[\text{Si}]_A$ . Each sample contained 100 layers, except sample SA3M56 which contained 60 layers.

Sample	$\delta$ -plane spacing (Å) (SIMS)	$[\text{Si}]_A$ (SIMS)		$\text{Si}_{\text{TOT}}$	Si concentration ( $10^{12} \text{ cm}^{-2}$ )				Hall ( $10^{12} \text{ cm}^{-2}$ ) ( $n_H$ )
		( $10^{12} \text{ cm}^{-2}$ )	(ML)		$\text{Si}_{\text{Ga}}$	$\text{Si}_{\text{As}}$	$\text{Si}_{\text{Ga}^-}\text{Si}_{\text{As}}$	Si-X	
SA2M12	485	6.0	0.01	5.5	5.5				1.7
SA10M54	460	6.1	0.01	10 <sup>a</sup>	10				3.9
SA2M09	420	14	0.02	9	9				6.5
SA10M55	490	16	0.02	15 <sup>a</sup>	15			4	5.0
MV1340	370	21	0.03	27	15	4	5	3	4.0
MV1342	385	35	0.05	26	12	4	3	7	3.2
SA10M57	475	59	0.09	29	14	5	3	7	3.0
MV1347	520	82	0.12	37	12	9	4	12	11
SA2M10	560	160	0.24	5	5				0.9
SA10M56	500	175	0.26	40	9	9	8	14	0.5
SA3M56	470	340	0.50	N.D.					0.4

<sup>a</sup>Electron irradiated to a dose of  $10^{18} e^- \text{ cm}^{-2}$ .

the covalent radii of the elements given by Pauling,<sup>25</sup> but these values are inconsistent with those obtained by recent *ab initio* local-density-functional calculations.<sup>26,27</sup> Simulations of the x-ray data for both 004 and 002 reflections have therefore been reinvestigated for various models using either the Pauling data or the calculated bond lengths.

The organization of the paper is follows. In Sec. II, details of the samples and the experimental procedures are discussed. In Sec. III, IR results for  $\delta$ -doping superlattices with various values of  $[\text{Si}]_A$  are described. IR and Raman data for dilute  $\delta$  layers with various interplanar spacings are presented in Sec. IV, together with data for highly homoge-

neously doped samples. Following analyses of simulations of x-ray data in Sec. V, an overall discussion, including *DX* behavior and likely diffusion processes occurring during growth, is given in Sec. VI. Our conclusions are set out in Sec. VII. Accounts of some of this work have been included in conference proceedings.<sup>28,29</sup>

## II. EXPERIMENTAL DETAILS

The MBE layers labeled SA (Tables I and II) were grown in a VG V80 system at Imperial College on semi-insulating (SI) liquid-encapsulated Czochralski (001) substrates and the

TABLE II. Si  $\delta$  superlattices with  $[\text{Si}]_A=0.01$  ML with various interplanar spacings.

Sample	Spacing ( $\delta$ -plane ML)	Intended No. of $\delta$ planes	$[\text{Si}]$ ( $10^{18} \text{ cm}^{-3}$ )	Mobility hall ( $\text{cm}^2/\text{V s}$ )	Carrier concentration ( $10^{18} \text{ cm}^{-3}$ )		$[\text{Si}]$ from Raman/IR absorption ( $10^{18} \text{ cm}^{-3}$ )				$\text{Si}_{\text{TOT}}$ ( $10^{18} \text{ cm}^{-3}$ ) (Raman /IR)	Missing Si ( $10^{18} \text{ cm}^{-3}$ ) (Raman /IR)	
					$n_R$	$n_H$	Si-X	$\text{Si}_{\text{Ga}^-}$	$\text{Si}_{\text{As}}$	$\text{Si}_{\text{Ga}}$			
SA7M26	1	500	212 <sup>a</sup>			b	16	8	9	32	65 <sup>c</sup>	147 <sup>c</sup>	
							55	17	44	65	181 <sup>d</sup>	31 <sup>d</sup>	
SA7M27	2	400	106 <sup>e</sup>	250		b	6.3	8	3	6	29	46	60
								24	10	20	39	93	13
SA7M28	5	400	39 <sup>a</sup>	489	20	13.5					20	20	19
											20	20	19
SA7M29	10	200	21 <sup>e</sup>	767	15.4	14					15	15	6
											16	16	5
SA7M35	20	200	12 <sup>a</sup>	894	10	9.3					11	11	1
											8	8	4
SA7M33	50	200	4.2 <sup>e</sup>	1431	3.7	3.9					3.3	3.3	0.9
											4.0	4.0	0.2
SA7M34	200	200	1.2 <sup>a</sup>	2707		0.86					1.5	1.5	-0.3

<sup>a</sup>SIMS data used to calibrate all of the samples.

<sup>b</sup>See text.

<sup>c</sup>Raman data.

<sup>d</sup>IR data.

<sup>e</sup>Estimated values taking account of SIMS data.<sup>a</sup>

TABLE III. Raman measurements of homogeneously doped GaAs:Si grown at 350 °C. Total Si concentrations calculated from  $[\text{Si}]_{\text{TOT}} = [\text{Si}_{\text{Ga}}] + [\text{Si}_{\text{As}}] + [\text{Si}_{\text{Ga-Si}_{\text{As}}}] + [\text{Si-X}]$ , and net donor concentration  $[N_D - N_A]$  set equal to  $[\text{Si}_{\text{Ga}}] - [\text{Si}_{\text{As}}] - [\text{Si-X}]$ ; both measured by LVM Raman spectroscopy.  $n_R$  is determined by Raman spectroscopy of coupled plasmon-phonon modes ( $\omega_+$ ). RT is room temperature.

Sample	SIMS ( $10^{18} \text{ cm}^{-3}$ )	$[\text{Si}]_{\text{TOT}}$ ( $10^{18} \text{ cm}^{-3}$ )	$N_D - N_A$ ( $10^{18} \text{ cm}^{-3}$ )	$n_R$ ( $10^{18} \text{ cm}^{-3}$ )	$n_H$ (RT) ( $10^{18} \text{ cm}^{-3}$ )
U4067	26	10.5	10.5	15	17
U4068	60	16.8	14.5	19	20
U5032		18.0	13.8	15	
U4069	85	26.1	12.3	20	18
U4073	130	33.0	10.8	20	19

reflection high-energy electron-diffraction (RHEED) oscillation technique was used prior to growth to calibrate the Ga flux. A buffer layer 1000 Å in thickness was grown at 580 °C, after which the substrate temperature was lowered to 400 °C and a  $c(4 \times 4)$  surface was observed by RHEED. Si was deposited to the required value of  $[\text{Si}]_A$ , while the Ga flux was interrupted but the As flux was maintained. The Si cell, held at 1250 °C, produced a flux equivalent to  $6 \times 10^{11} \text{ cm}^{-2} \text{ s}^{-1}$  determined from SIMS measurements of Si concentrations in homogeneously doped MBE layers. This sequence was repeated many times to fabricate the doping superlattice structures. The first set of samples (Table I) had  $\delta$  layers all separated from each other by a nominal 500 Å of undoped GaAs, and each  $\delta$  layer incorporated the same value of  $[\text{Si}]_A$ . Samples labeled *MV* were grown at the Philips Research Laboratories (Redhill, U.K.) in a modified Varian-360 system, and were used in our previous studies.<sup>3</sup> The second set of samples (Table II) comprised doping superlattices with various interplanar separations, and all layers had  $[\text{Si}]_A = 6 \times 10^{12} \text{ cm}^{-2}$  (0.01 ML).<sup>23</sup> The samples listed in Table III were grown at 350 °C, and were homogeneously doped with silicon in concentrations up to  $10^{20} \text{ cm}^{-3}$ .

Electrical measurements (300 K) were made on unprocessed van der Pauw samples and on standard Hall bar samples. The layers with a high carrier concentration required a well-defined contact geometry due to the small voltages and low mobilities. Ohmic contacts were made by annealing either indium or a Au/Ge/Ni alloy. Shubnikov-de Haas (SdH) measurements were also made at 4 K using an 8-T magnet<sup>23</sup> for the samples listed in Table II. The samples with  $\delta$  spacings of 200–50 ML showed miniband transport and two-dimensional (2D) effects, and it was apparent that the Hall data underestimated the true values of  $n$  by a factor of up to 2. As the interplanar spacing was reduced further, states occupied by electrons became characteristic of three-dimensional homogeneous doping (see also Ref. 24). The average volume concentration of carriers was therefore evaluated and compared with the intended doping level, assuming that all the Si impurities were present as  $\text{Si}_{\text{Ga}}$  donors, and that there was no compensation from intrinsic defects (Fig. 1). A value of  $n_{\text{max}} = 1.3 \times 10^{19} \text{ cm}^{-3}$  was obtained for the sample with 5-ML spacings, but there was a huge reduction from the expected carrier concentrations ( $n$  fell to a value close to zero) for the sample with the layer spacing of only 1 ML. No explanation of this decrease was given previously,<sup>23</sup> although persistent photoconductivity was de-

tected when samples held at 4.2 K were illuminated by an IR light-emitting diode: the increase in  $n$  was, however, only a few percent. There is therefore evidence that some *DX* centers were present, and were responsible in part for the electrical compensation. As the separation of the layers decreased, there was a monotonic decrease in the Hall mobility from  $2700 \text{ cm}^2/\text{V s}$  (200-ML sample) to  $250 \text{ cm}^2/\text{V s}$  for the 2-ML sample, leading to difficulties in making SdH measurements.

IR transmission spectra were obtained with a Bruker IFS 120HR interferometer with an instrumental resolution of  $0.25 \text{ cm}^{-1}$ , while the sample was held at a temperature close to 10 K, and a liquid-helium bolometer with a Ga-doped silicon element was used as the detector. The back of each sample was polished to give an overall wedge shape to avoid the occurrence of interference fringes in the recorded transmission spectrum ( $T_S$ ). An interferogram was first obtained without a sample in the beam to give the system spectral response ( $T_O$ ), and we then evaluated the quantity  $A_s = -\ln[T_S/T_O]$ . A similar procedure carried out with a wedged reference sample of undoped GaAs allowed  $A_R = -\ln[T_R/T_O]$  to be computed. The difference  $(A_s - \beta A_R) = A_D$  was then calculated, where the parameter  $\beta$  ( $\approx 1$ ) was adjusted to allow for small differences in the

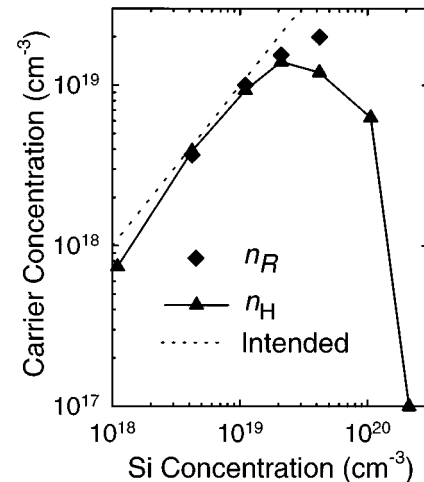


FIG. 1. The measured carrier concentrations  $n_H$  (Hall, 300 K) and  $n_R$  (coupled phonon-plasmon) for Si  $\delta$ -layer superlattice structures with  $[\text{Si}]_A = 6 \times 10^{12} \text{ cm}^{-2}$  (0.01 ML) with various interplanar spacings (Table II). Also shown are the intended Si concentrations.

thicknesses of the two (wedge-shaped) samples, so that absorption features due to intrinsic two-phonon processes were removed from  $A_D$  after the very large expansion required to reveal weak LVM lines. The absorption coefficients of the LVM's were obtained from  $\alpha = A_D/d$ , where  $d$  was the thickness of the epitaxial layer.<sup>30</sup> It should be noted that accurate values of the background absorption were not required in these studies. The free-carrier continuum absorption was removed from spectra by subtracting a smooth curve derived from a polynomial, usually of order 3. With scanning periods of up to 20 h, high signal-to-noise ratios were obtained, significantly superior to those obtained previously with a Bruker IFS 113v interferometer.<sup>3</sup>

For the samples listed in Tables II and III, Raman measurements were performed in the backscattering geometry from the (001) growth surface with the polarizations of the incident and scattered light parallel to two orthogonal  $\langle 001 \rangle$  crystallographic directions  $[z(x,y)\bar{z}]$ . The spectra were excited with the 3.00-eV line of a  $\text{Kr}^+$ -ion laser to produce resonantly enhanced scattering by the  $\text{Si}_{\text{Ga}}$  LVM (Ref. 31) with the samples cooled to 77 K. For crystalline GaAs, the probing depth  $1/(2\alpha_L)$  is 10 nm,<sup>32</sup> where  $\alpha_L$  denotes the absorption coefficient of the 3.00-eV radiation. The scattering light was dispersed by a triple monochromator, and detected with a liquid-nitrogen-cooled silicon charge-coupled detector array. This detector has a much better signal-to-noise performance than the sensitized diode array used in some earlier measurements.<sup>4,9</sup> The spectral resolution was  $\sim 2.5 \text{ cm}^{-1}$ . The free-carrier concentrations  $n_R$  (Raman) (Table II) were deduced from the measured frequencies of the coupled plasmon-phonon mode  $\omega_+$  by treating the electrons as a three-dimensional gas, to agree with the published transport data.<sup>23</sup>

### III. A REAPPRAISAL OF IR SPECTRA FROM HIGHLY $\delta$ -DOPED SUPERLATTICES

Previously examined samples (labeled *MV* in Table I) were remeasured, and additional IR LVM spectra (see Sec. II) are shown in Fig. 2. For values of  $[\text{Si}]_A$  less than  $\sim 0.03 \text{ ML}$ , only the LVM from  $\text{Si}_{\text{Ga}}$  was detected, and there were indications of a Fano interaction<sup>33,34</sup> with the free-carrier absorption (subtracted in the spectra shown). As  $[\text{Si}]_A$  was increased, there were initial increases in the integrated absorption (IA) coefficient of the  $\text{Si}_{\text{Ga}}$  LVM, but its strength then saturated and subsequently fell to zero for  $[\text{Si}]_A \sim 0.5 \text{ ML}$ , in agreement with the earlier observations (Fig. 3). However, lines from  $\text{Si}_{\text{As}}$ ,  $\text{Si}_{\text{Ga}}\text{-Si}_{\text{As}}$  pairs, and the Si-X complex were also present in the spectra for  $0.03 \leq [\text{Si}]_A < 0.5 \text{ ML}$  (Fig. 2), and showed a similar dependence on  $[\text{Si}]_A$  as the line from  $\text{Si}_{\text{Ga}}$ . These lines were much broader than that from  $\text{Si}_{\text{Ga}}$  (see Sec. I and also Ref. 3). The observations are in accord with corresponding spectra obtained from samples labeled *SA* (Table I), and also with our recent Raman-scattering data obtained from samples containing single  $\delta$  layers (see Fig. 2 in Ref. 13), except that the LVM from the Si-X defect was more prominent in the IR spectra: this difference is likely to be due to differences in the relative dipole moments and polarizabilities of the various modes. An important difference, however, is the absence in the IR spectra of the broadband near  $470 \text{ cm}^{-1}$  (line A)

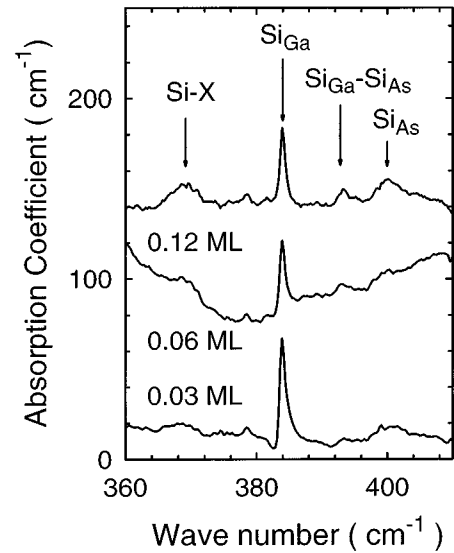


FIG. 2. IR-absorption spectra showing Si LVM's in the  $\delta$ -layer superlattices labeled *MV* (Table I) after subtraction of two-phonon intrinsic absorption from GaAs and free-carrier absorption: note the emergence of lines from  $\text{Si}_{\text{As}}$ ,  $\text{Si}_{\text{Ga}}\text{-Si}_{\text{As}}$  pairs, and Si-X when  $[\text{Si}]_A \geq 0.06 \text{ ML}$ . Spectra obtained previously from the same samples (Ref. 3) showed only the sharp line from  $\text{Si}_{\text{Ga}}$ . For  $[\text{Si}]_A \geq 0.5 \text{ ML}$ , no LVM lines were detected (see also Fig. 3).

(see Fig. 2 in Ref. 13). It is therefore confirmed that the associated dipole moment must be small. We emphasize that the Raman feature (line A) is not due to isolated  $\text{Si}_{\text{Ga}}\text{-Si}_{\text{As}}$  pair defects that give rise to sharp IR-absorption lines at  $464 \text{ cm}^{-1}$  ( $\Gamma_1$  symmetry) and at  $393 \text{ cm}^{-1}$  ( $\Gamma_3$  symmetry,  $C_{3v}$ ).<sup>35</sup> Line A must therefore be due to the vibrations of covalently bonded Si atoms present as small two-dimensional clusters. Since the line sharpens and shifts to higher frequencies as  $[\text{Si}]_A$  increases, it is inferred that the Si clusters increase in size.

Estimates of the concentrations of substitutional Si atoms in GaAs were deduced from established calibrations of the strengths of their LVM's (Refs. 36) for both the IR and Ra-

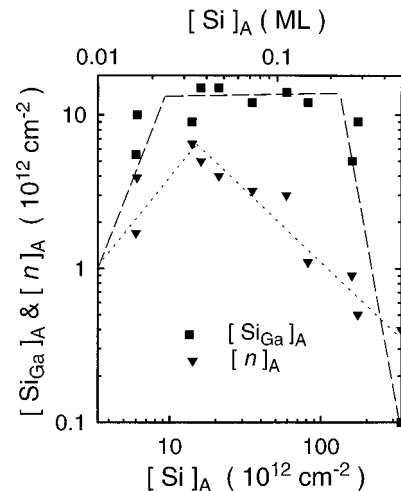


FIG. 3. Variation of the areal concentrations of  $\text{Si}_{\text{Ga}}$  and  $n$  (per layer) as a function of  $[\text{Si}]_A$  for all samples listed in Table I.

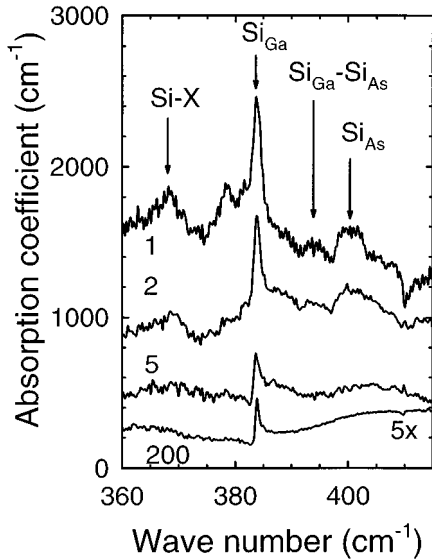


FIG. 4. IR absorption showing Si LVM's after removal of the free-carrier background and expansion of the vertical scale. For an interlayer spacing of 200–5 ML (Table II), only  $\text{Si}_{\text{Ga}}$  donors are detected with weak Fano asymmetries arising from interactions with the free-carrier continuum. For the 2- and 1-ML structures, lines from  $\text{Si}_{\text{As}}$ ,  $\text{Si}_{\text{Ga}}\text{-Si}_{\text{As}}$  pairs, and Si-X defects are present. For the 1-ML structure, there could be another absorption feature at  $376\text{ cm}^{-1}$ , as discussed in the text.

man measurements. For the donor an IR-integrated absorption coefficient  $IA$  equal to  $1\text{ cm}^{-2}$  corresponds to  $[\text{Si}_{\text{Ga}}]=5\times 10^{16}\text{ cm}^{-3}$  (a similar value is found for  $\text{Si}_{\text{As}}$  acceptors, but calibrations for the other lines are much less certain): the Raman calibration relating the scattering intensity to  $[\text{Si}_{\text{Ga}}]$  is given in Ref. 37, and it is assumed that the same calibration can be applied to the lines from  $\text{Si}_{\text{As}}$ ,  $\text{Si}_{\text{Ga}}\text{-Si}_{\text{As}}$  pairs, and the Si-X defect. The validity of these assumptions appears to be justified, because the ensuing predictions have been found to be in good agreement with other available estimates of concentrations (IR, SIMS, Hall effect) for a wide range of samples with  $[\text{Si}]<10^{19}\text{ cm}^{-3}$ . These estimates indicate that an increasingly large fraction of the deposited Si did not give rise either to IR absorption (Table I) or to Raman scattering (Ref. 13) for the range  $0.05\text{ ML}\leq[\text{Si}]_A\leq 0.5\text{ ML}$ . Some of these “missing” atoms may also be present as clusters of covalently bonded Si atoms that are smaller than the clusters that give rise to a detectable line A in the Raman spectra. Such a conclusion would not be incompatible with the data shown in Fig. 2 in Ref. 13, since the strength of line A, extrapolated linearly to lower values of  $[\text{Si}]_A$ , does not fall to zero until  $[\text{Si}]_A$  approaches zero.<sup>13</sup>

#### IV. IR AND RAMAN RESULTS FOR DILUTE $\delta$ LAYERS

##### A. Infrared measurements

After the subtraction of the two-phonon and free-carrier absorption, weak LVM's were detected in IR spectra for the samples listed in Table II (Fig. 4). For  $\delta$ -layer spacings  $>2\text{ ML}$ , only the  $\text{Si}_{\text{Ga}}$  local mode ( $384\text{ cm}^{-1}$ ) was observed as a slightly asymmetric Fano profile.<sup>33,34</sup> After irradiation of the 100-ML sample with 2-MeV electrons (at room tempera-

ture) to introduce traps that remove free carriers, this LVM assumed a symmetrical shape, and a small line due to  $^{29}\text{Si}_{\text{Ga}}$  (4.7% abundant) was just detected at  $379\text{ cm}^{-1}$ : no other Si LVM's were detected. The  $^{28}\text{Si}_{\text{Ga}}$  LVM in the samples with 2- and 1-ML spacings (with intended volume doping levels of  $10^{20}$  and  $2\times 10^{20}\text{ cm}^{-3}$ , respectively) was symmetrical (without a prior irradiation) due to the low concentrations of free carriers. Of primary significance, however, was the emergence of additional LVM's from  $\text{Si}_{\text{As}}$  ( $399\text{ cm}^{-1}$ ),  $(\text{Si}_{\text{Ga}}\text{-Si}_{\text{As}})$  pairs ( $393\text{ cm}^{-1}$ ) and Si-X ( $367\text{ cm}^{-1}$ ) for these two layers, indicating that self-compensation had occurred. It is surprising that this did not occur for the 5-ML sample, since the intended doping level ( $4\times 10^{19}\text{ cm}^{-3}$ ) is double that expected for the onset of DX behavior when the position of the Fermi level is close to  $\sim(E_c+200\text{ meV})$  (Ref. 38) at zero pressure. There was again an indication that some of the silicon was not detectable by IR absorption (Table II).

A possible absorption feature at  $\sim 376\text{ cm}^{-1}$  in the spectrum of the 1-ML sample was not reproduced in further measurements on a range of samples. This comment is made only because of the work of Wolk *et al.*,<sup>39</sup> who measured LVM spectra of Si-doped GaAs at 5 K under a high hydrostatic pressure, and found a line that they attributed to the Si (DX) center: their extrapolation of the frequency to zero pressure yielded a value of  $376\pm 1.5\text{ cm}^{-1}$ , the same as that shown in Fig. 4. It is most likely that our observation is spurious.

##### B. Raman measurements

The samples with  $\delta$  spacings from 5 to 50 ML showed a well-resolved high-frequency-coupled plasmon-phonon mode  $\omega_+$  (Fig. 5). Use of a procedure described in Ref. 40, together with the measured frequencies of  $\omega_+$ , allowed values of the carrier density ( $n_R$ ) to be obtained (Table II). The broadening of  $\omega_+$  modes as the layer separation decreased was due to reductions in the carrier mobility. For the 2- and 1-ML samples, the  $\omega_+$  mode could not be detected probably because too large a broadening was caused by further reductions in the mobility, but observed scattering by the low-frequency-coupled plasmon-phonon mode  $\omega_-$  (Fig. 6) indicated that some conduction electrons were present. In principle, the measured strength of the  $\omega_-$  mode relative to that of the unscreened LO-phonon line originating from the surface depletion region can be used to obtain a semiquantitative estimate of  $n_R$ . Thus there appeared to be more electrons present when samples were illuminated by the 3.00-eV laser light than when they were in the dark, implying photoexcitation from traps.

Raman scattering from Si LVM's after subtraction of intrinsic two-phonon features is shown in Fig. 7. For layers with separations down to and including 5 ML, only the line from  $\text{Si}_{\text{Ga}}$  donors was detected. For the 2-ML sample, additional lines from  $\text{Si}_{\text{As}}$ ,  $\text{Si}_{\text{Ga}}\text{-Si}_{\text{As}}$  pairs, and Si-X were clearly visible. These additional lines were stronger in relation to the  $\text{Si}_{\text{Ga}}$  line in the 1-ML sample, but there was no clear indication of a feature at  $376\text{ cm}^{-1}$  (cf. Fig. 4). Of particular significance, however, was the absence of a detectable vibrational band A at  $\bar{\nu}\geq 480\text{ cm}^{-1}$ , due to covalently bonded Si

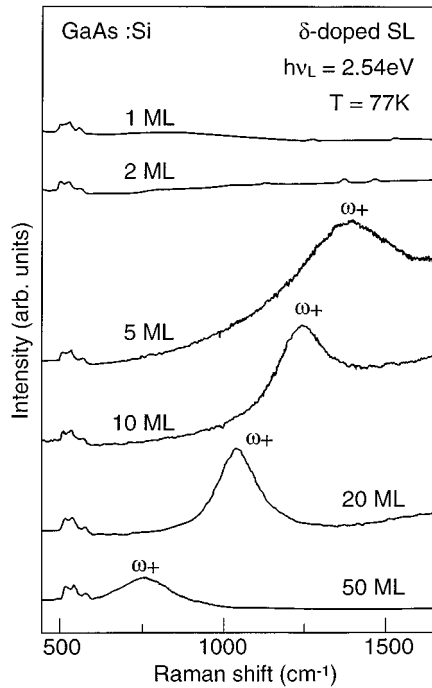


FIG. 5. Raman spectra showing scattering from the  $\omega_+$  coupled phonon-plasmon mode that shifts to higher energies as the interlayer spacing of  $\delta$ -layer superlattices (Table II) is decreased from 50 to 5 ML. The mode is not detected in samples with 1- and 2-ML spacings.

clusters, and another indication that not all the Si atoms were detected by their LVM scattering.

The results described in Secs. IV A and IV B are comparable in every way to those obtained for the homogeneously Si-doped samples listed in Table III. For intended doping concentrations with  $[\text{Si}] \leq 4 \times 10^{19} \text{ cm}^{-3}$ , only the  $\text{Si}_{\text{Ga}}$  LVM was detected, but at the higher doping levels the full range of Si-related centers was observed. Raman spectra were much superior to IR spectra, which showed strong free-carrier absorption. Raman measurements were also made of the coupled plasmon-phonon mode  $\omega_+$  to determine the carrier concentrations given in Table III, together with the estimates of the total amounts of Si that gave rise to the LVM's. It was implied that only some 50% of the total Si was present in complexes involving substitutional Si atoms in GaAs (cf. Table II), but again line A was not detected in Raman spectra.

Thus 2D Si clusters were detected only when the Si atoms were deposited in close proximity to each other in a  $\delta$  layer with a large value of  $[\text{Si}]_A \geq 0.5 \text{ ML}$ . Nevertheless, we show in Sec. VI that these observations do not preclude the possibility that long-range bulk diffusion may have occurred during overgrowth of the  $\delta$  layers.

## V. X-RAY CHARACTERIZATION OF $\delta$ LAYERS

An x-ray-diffraction profile from a periodic doping superlattice includes satellite peaks around the Bragg peak for the average structure, and the separation of this zero-order satellite from the GaAs substrate peak depends on the average strain in the layer structure.<sup>41</sup> The satellites are interference

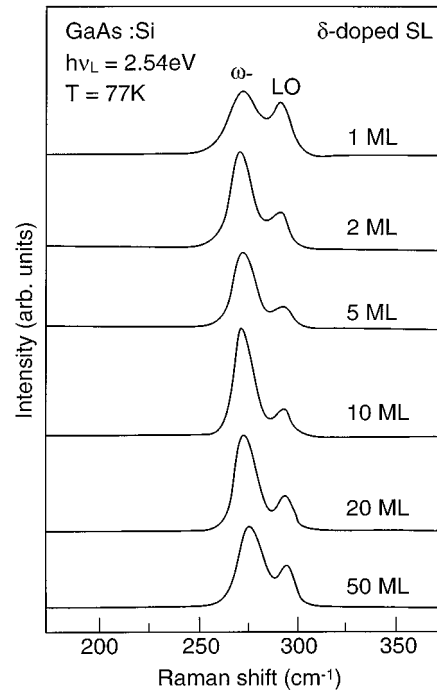


FIG. 6. Raman spectra showing scattering from the  $\omega_-$  coupled phonon-plasmon mode from  $\delta$ -layer superlattices (Table II) as a function of the interlayer spacing. Note that the mode is still detected for the 1- and 2-ML spacings, even though the  $\omega_+$  mode is not observed.

fringes arising from the phase shift between adjacent GaAs “spacer” layers separated by the thin  $\delta$  layers. The satellite intensities depend on the amplitude of the composition modulation, arising from (a) changes in the bond lengths in the  $\delta$  layer and (b) differences between the scattering factors of the atoms in the  $\delta$  layers and the Ga and As atoms that they replace. Simultaneous modulation of these two quantities introduces an asymmetry into the satellite intensities about the zero-order peak (Figs. 8 and 9) (see also Figs. 1 and 2 of Ref. 12). “Allowed” reflections such as 004 are sensitive primarily to strain modulation, whereas “forbidden” reflections such as 002 (occurring only because of the difference between the Ga and As scattering factors) are sensitive to structure factor modulation. The satellite intensities are proportional to the square of the Fourier coefficients of the composition modulation. The highest-order satellites are the most sensitive to the interface shape, and most of this scattering comes from regions close to the interfaces. A rectangular modulation with abrupt interfaces will give the maximum number of satellites. Variations in the period cause a broadening of the satellite peaks that increases with satellite order, although the integrated intensities do not change. A detailed analysis of a Si  $\delta$  structure can be made only if there is a large number (50–100) of  $\delta$  layers in a stack with a regular period, and if  $[\text{Si}]_A$  is greater than  $\sim 0.3 \text{ ML}$ ,<sup>15</sup> so that the satellites are visible above the background noise using an instrument with a dynamic range of  $10^6$ . We have found that the inclusion of this number of layers with  $[\text{Si}]_A \geq 1.0 \text{ ML}$  leads to the introduction of dislocations or surface undulations (strain and thickness fluctuations) to relieve the strain in samples grown under the con-

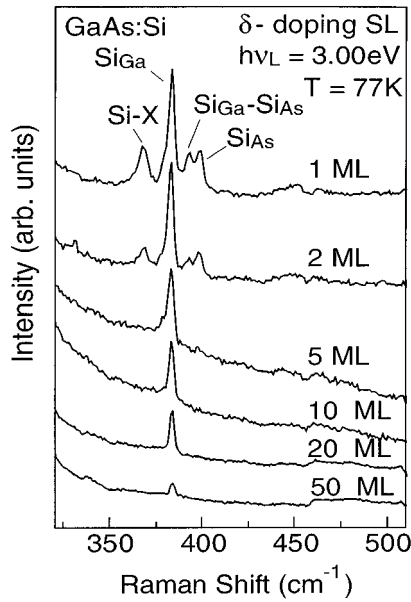


FIG. 7. Raman spectra showing scattering from Si LVM's in  $\delta$ -doping superlattices (Table II) as a function of the interlayer spacing. Only the mode from  $\text{Si}_{\text{Ga}}$  is detected for spacings in the range 50–5 ML. The samples with spacings of 1 and 2 ML show, in addition, LVM's from  $\text{Si}_{\text{As}}$ ,  $\text{Si}_{\text{Ga-SiAs}}$  pairs, and the Si-X defect, in agreement with the IR data (Fig. 4). There is no detectable feature at  $376 \text{ cm}^{-1}$  in the sample with the 1-ML  $\delta$  spacing.

ditions specified in Sec. II (see Fig. 10). This mode of strain relief has been demonstrated previously for the growth of SiGe alloys on (001) Si,<sup>42,43</sup> and for  $\text{In}_x\text{Ga}_{1-x}\text{As}$  on GaAs.<sup>44</sup> There is therefore only a narrow range of  $[\text{Si}]_A$  for which meaningful measurements can be obtained. Within this range, the average spacing of the  $\delta$ -doping superlattice, the strain, and the average spreading of the  $\delta$  layers can be determined.

To fit the measured 004 diffraction profile (Fig. 8), a structure incorporating 60  $\delta$  layers, each with  $[\text{Si}]_A = 0.5$  ML, corresponding to a notional thickness of  $1.4 \text{ \AA}$  but with

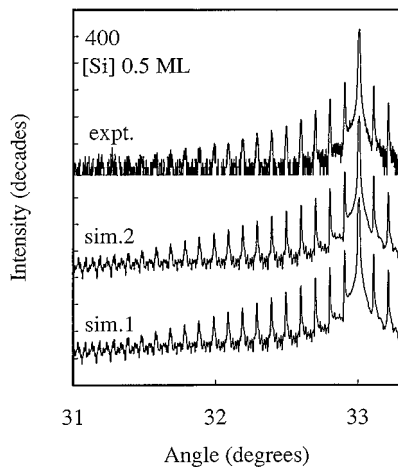


FIG. 8. 004 x-ray-diffraction profiles: expt., experimental data; sim.1, original simulation for 60 periods of  $515 \pm 15 \text{ \AA}$  for  $(\text{Si}_{0.5}\text{Ga}_{0.5})(\text{V}_{0.125}\text{As}_{0.875})$  (see Ref. 12); sim.2, new simulation  $(\text{Si}_{0.25}\text{Ga}_{0.5}\text{As}_{0.125}\text{V}_{0.125})(\text{Si}_{0.25}\text{As}_{0.75})$ .

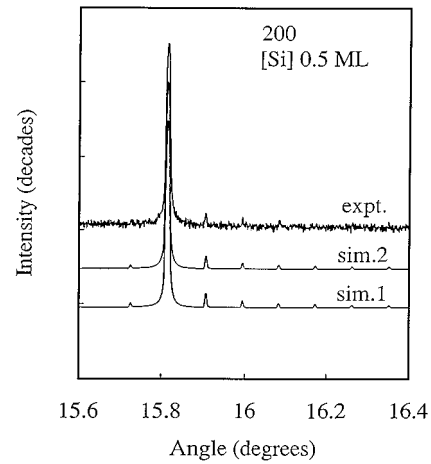


FIG. 9. 002 x-ray-diffraction profiles: expt., experimental data; sim.1, original simulation for 60 periods of  $515 \pm 15 \text{ \AA}$  for  $(\text{Si}_{0.5}\text{Ga}_{0.5})(\text{V}_{0.125}\text{As}_{0.875})$  (see Ref. 12); sim.2, new simulation  $(\text{Si}_{0.25}\text{Ga}_{0.5}\text{As}_{0.125}\text{V}_{0.125})(\text{Si}_{0.25}\text{As}_{0.75})$ .

spreading over no more than 2 ML ( $5.4 \text{ \AA}$ ), requires a strain of 3.7% and a spacing of  $515 \pm 15 \text{ \AA}$ . For a pseudomorphic structure with a tetragonal distortion, the strain in the growth direction has to be multiplied by the factor  $(1 + \nu)/(1 - \nu) \approx 2$ , where  $\nu$  is Poisson's ratio (equal to 0.31 for GaAs and 0.28 for Si).<sup>45</sup> To carry out the simulations, it is also necessary to know the Debye-Waller factors (equal to 0.67 for GaAs and 0.50 for Si),<sup>46</sup> that lead to reductions in the x-ray intensities and peak widths. The required strain can be simulated by assuming that all Si atoms occupy Ga-lattice sites in one plane (50% substitution), that As atoms occupy all the group-V lattice sites in the next layer, and that Vegard's law is valid, and using the Pauling covalent radii (Table IV). To achieve a satisfactory simulation of the 002 reflection (Fig. 9) it is necessary, however, to reduce the scattering from the As layer. This was modeled previously by allowing As vacancies ( $V_{\text{As}}$ ) to be present ( $\text{V}_{0.125}\text{As}_{0.875}$ ) (Fig. 9), but this was not deemed to be a satisfactory solution as the

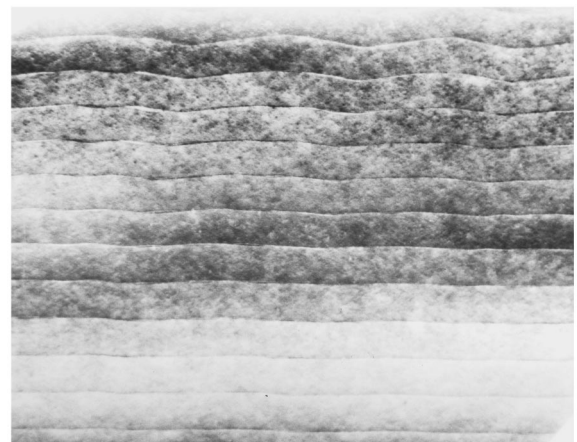


FIG. 10. Dark-field TEM micrograph showing a cross section of a sequence of  $\delta$  layers each with  $[\text{Si}]_A = 1 \text{ ML}$  and spaced by  $500 \text{ \AA}$  in a GaAs superlattice comprising 30 layers. After the growth of 14 layers, the growth surface becomes nonplanar to relieve the increasing strain; subsequent  $\delta$  layers then show a zigzag structure.



TABLE IV. Bond lengths.

Complexes	Bond length (Å)	
	Ref. 25	Ref. 26
Si-As	2.35	2.45
Si-Ga	2.43	2.36
Si-Si	2.34	2.38
Ga-As	2.44	

layers were grown under As-rich conditions. An alternative possibility of locating Si atoms on As lattice sites gave marginally inferior fits to the 004 diffraction profile, but required  $[\text{Si}]_A$  to be increased above the value measured by SIMS. For example, a good fit was obtained by replacing the Ga layer by  $\text{Si}_{0.5}\text{Ga}_{0.5}$ , and the next As layer by  $\text{Si}_{0.25}\text{As}_{0.75}$ . If instead, recently calculated bond lengths<sup>26</sup> are used (Table IV), the compositions of the two layers would have to be changed to  $\text{Si}_{0.25}\text{Ga}_{0.75}$  and  $\text{Si}_{0.5}\text{As}_{0.5}$ , respectively, to model the 004 reflection, but this model is unsatisfactory because the asymmetry of the 002 satellites is then in the opposite sense to that measured. To fit the 002 diffraction profile, the average scattering factor for the atoms occupying As lattice sites has to be approximately 25% greater than that of the atoms occupying Ga lattice sites.

Since LVM's from Si atoms in solution in GaAs or line A (see Fig. 2 in Ref. 13) for  $[\text{Si}]_A \approx 0.5$  ML were hardly detectable in the present Raman and IR measurements, the actual arrangement of the Si atoms is unknown. To proceed, we therefore first made use of the observations of the defects present in  $\delta$  layers with somewhat smaller values of  $[\text{Si}]_A$ . Assuming that Si-X is a  $V_{\text{Ga}}\text{-Si}_{\text{As}}\text{-As}_{\text{Ga}}$  defect (see Sec. VI), there would be a requirement for an original Ga layer to contain  $V_{\text{Ga}}$  and  $\text{As}_{\text{Ga}}$  defects, as well as Si and Ga atoms. By replacing the Ga layer by  $(\text{Si}_{0.25}\text{Ga}_{0.5}\text{As}_{0.125}\text{V}_{0.125})$ , and the adjacent As layer by  $\text{Si}_{0.25}\text{As}_{0.75}$ , it was possible to obtain a fit to the 004 and 002 reflections (Figs. 8 and 9), equally good to that shown in Fig 2 of Ref. 12, but only if calculated bond lengths<sup>26</sup> were used. The covalent bond lengths associated with complexed  $\text{As}_{\text{Ga}}$  and  $V_{\text{Ga}}$  are not known, and the strain arising from their combined presence was arbitrarily set equal to zero. In fact, the isolated  $\text{As}_{\text{Ga}}$  defect has a large radius according to theory,<sup>47,48</sup> while the  $V_{\text{Ga}}$  center is likely to be elastically ‘‘soft,’’ so that some compensation of the strain should occur. The model proposed could only be simulated by atomic substitutions spread over four atomic layers because of the limitations of the software. The model allowed  $[\text{Si}_{\text{Ga}}] + [\text{Si}_{\text{As}}] = 0.5$  ML (SIMS), and  $[V_{\text{Ga}}] = [\text{As}_{\text{Ga}}]$ , consistent with the requirement for the proposed structure of Si-X, while  $[\text{Si}]_{\text{As}}$  allowed equal concentrations of ‘‘isolated’’  $\text{Si}_{\text{As}}$  and Si-X defects to be present. Covalent bonding of  $\text{Si}_{\text{Ga}}$  and  $\text{Si}_{\text{As}}$  is possible because  $[\text{Si}_{\text{Ga}}] = [\text{Si}_{\text{As}}]$ . A physical interpretation is that 2D Si clusters are formed with GaAs present in the intervening regions. The insertion of equal concentrations of Si in both the Ga and As layers does not contribute to the intensities of the 002 satellites: These arise because of the assumption that  $V_{\text{Ga}}$  defects are present.

Finally, we point out that in other studies<sup>49,50</sup> of Si layers, thicker than 1 ML, x-ray profiles have been satisfactorily modeled by assuming that only Si atoms were present in the

layers, i.e., without vacancies or As atoms, although details of the bonding to adjacent Ga or As atoms were not taken into account.

In summary, there are severe constraints on models that can fit the observations. Although our earlier modeling based on the presence of  $\text{Si}_{\text{Ga}}$  was thought to be satisfactory, the more recent Raman data and the present IR data clearly require alternative models to be proposed, but the outcome is far from ideal. We can obtain an excellent fit to the measurements, but the model is not unique, and a further problem has arisen relating to the choice of covalent bond lengths.<sup>25,26</sup> It is clear that x-ray measurements taken in isolation do not provide sufficient information to allow the structure of the  $\delta$  layers to be determined.

## VI. DISCUSSION

Our earlier IR measurements<sup>3</sup> revealed only the LVM from  $\text{Si}_{\text{Ga}}$  donors in  $\delta$ -doping superlattices grown at 400 °C with interlayer spacings of 500 Å, but improved measurements (Secs. II and III) have shown that  $\text{Si}_{\text{As}}$ ,  $\text{Si}_{\text{Ga}}\text{-Si}_{\text{As}}$  pairs, and Si-X defects are also present as soon as  $[\text{Si}]_A$  is increased to  $\sim 2 \times 10^{13} \text{ cm}^{-2}$  (0.03 ML), consistent with Raman results.<sup>13</sup> At this value of  $[\text{Si}]_A$  the average volume carrier concentration  $n$  would be equal to  $\sim 2 \times 10^{19} \text{ cm}^{-3}$ , if all the Si atoms occupied Ga sites in a single plane, and the carriers were confined in a well with a width of  $\sim 100$  Å. This width is close to that calculated from a Poisson-Schrödinger self-consistent analysis,<sup>5</sup> although the depth of the well is strongly dependent on any spreading of the donors to sites immediately adjacent to the  $\delta$  plane. For our doping superlattices, the well width clearly could not exceed 500 Å, as this was the interlayer spacing. Parallel LVM results obtained by Raman scattering<sup>13</sup> from single  $\delta$  planes also imply that interactions between neighboring  $\delta$  layers in the doping superlattices examined here are unimportant.

Raman (see Fig. 2 in Ref. 13) and IR measurements (Fig. 2) lead to a further clarification. All LVM scattering and absorption from substitutional Si atoms in the GaAs matrix is lost once  $[\text{Si}]_A$  is increased above 0.5 ML. Raman scattering then shows the emergence of line A attributed to small covalently bonded 2D Si-like clusters. Associated IR absorption has not been detected, although it is predicted to occur according to *ab initio* local-density-functional theory.<sup>26</sup> Buried 2D clusters are also just detected in our high-resolution direct lattice transmission electron micrographs for  $[\text{Si}]_A \approx 0.5$  ML, and their presence can also be inferred from lattice tilts revealed by x-ray diffraction.<sup>15</sup> The IR and Raman measurements imply that all the Si atoms become incorporated into a  $\delta$  phase. *N*-type conductivity in the adjacent layers of GaAs is therefore not expected, unless electrons are derived from the  $\delta$  phase itself. Electrical measurements show that the conductivity of the doping superlattice falls to a value close to zero for  $[\text{Si}]_A \leq 0.5$  ML. The conclusion is that any conduction electrons present in the  $\delta$  phase do not diffuse into the GaAs. There is still a lack of conductivity even when  $[\text{Si}]_A$  is increased up to several layers, suggesting that the  $\delta$  layers themselves are nonconducting. Capacitance-voltage measurements made in much earlier work<sup>52</sup> on samples grown at 520 °C showed that the conductivity was lowered in planar regions immediately adjacent to and in-

cluding individual  $\delta$  layers when  $[\text{Si}]_A$  is as low as 0.015 ML, even though the conductivity was high in the GaAs matrix away from the  $\delta$  planes. Reexamination of SIMS profiles published in this same work<sup>52</sup> indicates that the  $\delta$  phase starts to be apparent as spikes in the Si concentration for  $\delta$  layers, with  $[\text{Si}]_A$  as low as 0.02 ML. The implication is that covalently bonded Si-Si was present at an early stage of the Si deposition, consistent with extrapolation from higher coverages of the present Raman data for line A, from STM (Ref. 20) observations of aggregation of Si atoms by surface diffusion, and from the low areal concentration of Si at the start of the plateau region shown in Fig. 3.

The measured frequency of the A line (Raman) implies the presence of Si-Si bonds, so that  $\delta$  layers must be essentially “Si like” rather than having a composition such as  $\text{Si}_3\text{As}_4$  (see Refs. 16 and 17), in which Si atoms are bonded only to As atoms. This conclusion is not unexpected, since experiments<sup>53</sup> and theoretical<sup>54</sup> studies demonstrate that impinging Si atoms displace As atoms present as a surfactant during the growth of silicon layers by solid-source molecular-beam epitaxy. Nevertheless, electrical measurements made on these Si layers indicated that there is some incorporation of As atoms<sup>53</sup> in the silicon, and so the present  $\delta$  layers might also have been expected to show *n*-type conductivity. The apparent discrepancy could be explained if electrons are trapped in midgap states at the interface of the  $\delta$  structure, similar to the mechanism proposed for the loss of electrons in low-temperature MBE (LTMBE) GaAs following the precipitation of metallic arsenic that occurs in post-growth anneals.<sup>55,56</sup> The surrounding GaAs is then semi-insulating. It has also been reported that bulk Si doped with As in a concentration of  $\sim 10^{21} \text{ cm}^{-3}$  has a much lower conductivity than expected due to As precipitation,<sup>57</sup> and an explanation based on the presence of silicon vacancies has been proposed<sup>58</sup> to explain this result. It is unclear whether these results have relevance to thin Si layers in GaAs, but further discussion is deferred until chemical analyses have been made of the composition of the present Si  $\delta$  layers.

The manner in which Si is incorporated into  $\delta$  layers is clearly radically different from that of Al, which continues to occupy only group-III lattice sites as  $[\text{Al}]_A$  is increased up to and beyond  $\sim 0.5$  ML. In this system, AlAs is formed, and the  $\text{Al}_{\text{Ga}}$  IR LVM seen in dilute  $\delta$  layers shifts in frequency and continues to increase in strength to become the TO like mode of another component, while the  $\text{Al}_{\text{Ga}}$  Raman LVM shifts to become the LO-like mode.<sup>18,59–61</sup>

Raman measurements made on dilute  $\delta$ -layer superlattices (Table II) agree with the IR LVM data. For layers with a separation greater than or equal to 5 ML, only the  $\text{Si}_{\text{Ga}}$  LVM was detected. At this separation, the volume concentration of  $[\text{Si}]$  would have reached  $\sim 4 \times 10^{19} \text{ cm}^{-3}$ , according to the intended and measured SIMS doping level. IR measurements indicated  $[\text{Si}_{\text{Ga}}] = 1.8 \times 10^{19} \text{ cm}^{-3}$ , while Raman measurements yielded  $[\text{Si}_{\text{Ga}}] = 2.0 \times 10^{19} \text{ cm}^{-3}$  and  $n_R = 2 \times 10^{19} \text{ cm}^{-3}$ .  $n_R$  (Raman) was larger than  $n_H$  (Hall)  $= 1.2 \times 10^{19} \text{ cm}^{-3}$ , that may be an underestimate<sup>22</sup> of the true value of  $n$ . The higher Raman values could be due to the photoexcitation of electrons from traps resulting from the incident laser illumination.<sup>62</sup> The different values of  $[\text{Si}_{\text{Ga}}]$  determined by the IR measurements on the one hand and the Raman technique on the other for smaller interplanar spac-

ings imply measurement errors, possibly due to different sampling depths of the illumination. There was a second discrepancy (a factor of 2) between the smaller measurement (LVM) value of  $[\text{Si}_{\text{Ga}}] = 2 \times 10^{19} \text{ cm}^{-3}$  compared with the actual doping level of  $4 \times 10^{19} \text{ cm}^{-3}$  for the 5-ML sample. A similar deficit was observed in very heavily homogeneously Si-doped (up to  $10^{20} \text{ cm}^{-3}$ ) GaAs grown at 350 °C (Table III).

It is important to recall that Raman feature A was not detected in any of these samples, but its detection limit for a Si  $\delta$  layer corresponded to  $[\text{Si}]_A = 0.5$  ML ( $3.4 \times 10^{14} \text{ cm}^{-2}$ ) for a Si sheet located 5 nm beneath the surface (see Fig. 2 in Ref. 13). If that amount of Si were distributed homogeneously within the probing depth (10 nm), the corresponding 3D detection limit would be about  $3 \times 10^{20} \text{ cm}^{-3}$ . This concentration is a factor of 4–5 times *greater* than that of the missing Si (of the order of  $5\text{--}7 \times 10^{19} \text{ cm}^{-3}$ ) in the most heavily doped GaAs/Si sample (Table III). It follows that if all these missing Si atoms were incorporated into covalently bonded Si-Si clusters, they would not be detectable by Raman spectroscopy. The alternative use of cross-sectional scanning tunneling microscopy has led to the detection of precipitates in homogeneously doped (001) MBE GaAs grown at 375 °C with  $[\text{Si}]$  at  $6 \times 10^{19} \text{ cm}^{-3}$ . The particles were oval shaped, with their long axes approximately 80 Å in length and orientated along the growth direction; their chemical composition was, however, not determined.<sup>63</sup> The possibility that these particles were small Si clusters and that similar clusters were formed in our samples cannot be discounted.

The available evidence from previous STM studies of (a) homogeneously doped material<sup>22</sup> and (b) surface deposits that are precursors to  $\delta$ -doping structures<sup>21</sup> indicates that Si impurity atoms deposited during MBE (001) GaAs growth, under the conditions used in the present work, all occupy Ga surface sites. Since such atoms are not fully bonded impurities in GaAs, it is not sensible to ascribe donor activity to them until they are covered by a layer of GaAs: even then, the surface layer is expected to be fully depleted due to the presence of surface states. Compensation does not occur for material grown at a low temperature (350–400 °C) if the resulting value of  $n_{\text{MAX}}$  at room temperature is smaller than  $\sim 2 \times 10^{19} \text{ cm}^{-3}$ . For layers with this doping level grown at higher temperatures, compensation is observed, due to the presence of  $\text{Si}_{\text{As}}$  acceptors,  $\text{Si}_{\text{Ga}}\text{-Si}_{\text{As}}$  pairs, and Si-X defects that must have been produced by silicon diffusion processes in the GaAs matrix beneath the surface. Measurements on homogeneously Si-doped GaAs grown at 400 °C,<sup>37</sup> and subsequently heated to 500 or 600 °C in the MBE equipment under an As-flux, support this proposal, since LVM measurements showed progressive site switching of  $\text{Si}_{\text{Ga}}$  donors to the other sites as the temperature was increased. Similar observations demonstrate that Si diffusion jumps also occur when these impurities are present in  $\delta$  layers.<sup>15</sup> For high values of  $[\text{Si}]_A$ , SIMS measurements reveal a uniform Si concentration of  $2 \times 10^{19} \text{ cm}^{-3}$  in the regions between adjacent  $\delta$  layers with much larger spikes close to  $10^{21} \text{ cm}^{-3}$  at the positions of the  $\delta$  phase. The rapid diffusion of the Si atoms out of the  $\delta$  layers<sup>15</sup> could be explained by the presence of negatively charged vacancies, thought to be  $V_{\text{Ga}}$  defects<sup>64</sup> that were detected by positron annihilation mea-

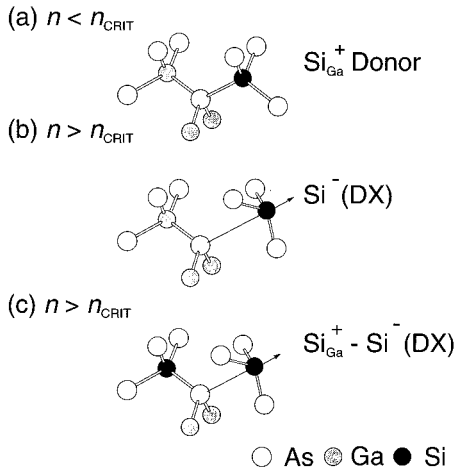


FIG. 11. The location of the Si impurity atom in the GaAs lattice: (a) as a donor atom occupying a substitutional tetrahedra Ga site; (b) in the  $DX$  configuration involving a displacement along a  $\langle 111 \rangle$  direction toward an adjacent vacancy (Ref. 21), as detected in samples at low temperatures with the application of a hydrostatic pressure; and (c) a proposed interchange of the Si ( $DX$ ) with a nearest-neighbor As atom occurring during growth to produce a  $Si_{As}$ - $As_{Ga}$  pair.

measurements made on our  $\delta$ -doping superlattices.

The discussion implies that there are diffusion jumps of Si atoms from Ga sites to adjacent interstitial sites,<sup>48</sup> or that there is an exchange of sites with neighboring As atoms. The former process would generate a  $V_{Ga}$  defect, and the latter a  $Si_{As}$ - $As_{Ga}$  nearest-neighbor pair.  $V_{Ga}$  defects would certainly diffuse, and trapping by the  $Si_{As}$ - $As_{Ga}$  pair would generate the Si-X defect ( $V_{Ga}$ - $Si_{As}$ - $As_{Ga}$ ). The structure for the Si-X center was, however, first proposed following its formation observed by IR LVM spectroscopy as second-neighbor  $Si_{Ga}$ - $V_{Ga}$  pairs were destroyed during anneals of LTMBE GaAs at 350 °C:<sup>14</sup> the transformation was attributed to two successive diffusion jumps, first of the bridging As atom and then the  $Si_{Ga}$  (see also Ref. 17). It is not certain that the Si-X defect incorporates an  $As_{Ga}$  defect, but contrast characteristic of these antisite defects has been observed in  $n$ -type layers of  $Al_xGa_{1-x}As$  examined by cross-section STM.<sup>65</sup> The various diffusion jumps described, involving the formation of  $V_{Ga}$  and  $Ga_{As}$  defects, could lead to a reorganization of the as-deposited Si atoms originally occupying Ga sites on the surface to the observed Si-like  $\delta$  layers, possibly as the result of the aggregation of Si interstitials.

Finally, we propose a mechanism that would be expected to lead to the onset of autocompensation in GaAs, so that  $n_{MAX}$  never exceeds the  $DX$  limit of  $\sim 2 \times 10^{19} \text{ cm}^{-3}$ , irrespective of the growth method or the growth temperature. Once  $n$  exceeds this value, there would be displacements of some  $Si_{Ga}$  toward adjacent interstitial sites,<sup>48</sup> leading to a severe weakening of the associated  $Si_{Ga}$ -As bonds (Fig. 11), thereby enhancing the probability that a diffusion jump takes place.<sup>66</sup> It has been shown by theory that  $DX$ -like behavior also occurs for second-neighbor  $Si_{Ga}$ - $Si_{Ga}$  pairs with a displacement of one  $Si_{Ga}$  away from its neighbor,<sup>67</sup> similar to that found for Si donors paired with other acceptors (Zn, Cu, etc.),<sup>68</sup> so that a single Si diffusion jump would lead to the formation of a  $Si_{Ga}$ - $V_{Ga}$  pair. As the temperature of the

sample is increased, either during growth or a subsequent anneal, the Fermi distribution would extend to higher energies in the conduction band, so that more  $DX$  centers would form and then be destroyed due to  $Si_{Ga}$  diffusion jumps. It follows that there would be corresponding increases in the compensation of samples.<sup>69,70</sup> These arguments do not in general explain the increasing degree of compensation as the Si doping level is increased, since the carrier concentration would always be expected to rise to some equilibrium value. Nevertheless, this latter behavior was found for our homogeneously doped samples grown at  $T_g = 350 \text{ }^\circ\text{C}$  (Table III).

## VII. CONCLUSIONS

It has been shown both by LVM Raman scattering and IR absorption that  $Si_{As}$ ,  $Si_{Ga}$ - $Si_{As}$  pairs, and the electron trap Si-X are all present in  $\delta$  layers grown at 400 °C, with  $[Si]_A$  greater than  $\sim 0.05$  ML. These measurements supersede previous IR measurements that revealed only the  $Si_{Ga}$  LVM's. These LVM's are no longer detected by either technique once  $[Si]_A$  is increased beyond  $\sim 0.5$  ML. The Raman measurements then show a high-frequency feature that is attributed to scattering from the vibrations of covalently bonded Si-Si pairs. This feature is not observed in IR spectra, and neither are other expected lines due to Si-Ga and Si-As vibrational modes. We have reviewed the interpretation of previous x-ray measurements made on superlattice structures, and have shown that modeling does not lead to the prediction of a unique structure. A layer containing Si-Si clusters and other defects is, however, a plausible alternative structure to the one incorporating only  $Si_{Ga}$  atoms. It is unclear whether the formation of Si-Si 2D clusters can occur by long-range diffusion, although such defects were not detected in samples containing dilute  $\delta$  layers with a small interplanar spacing or in homogeneously doped samples. The observed Si-Si 2D clusters (Raman line A) must therefore have resulted from the close proximity of Si impurities in highly doped  $\delta$  layers that resulted from surface diffusion or by local diffusion jumps of Si atoms during the overgrowth of more GaAs. The Si-like clusters appear to be relatively stable, but may incorporate As atoms and vacancies. The presence of the latter defects and/or interface states could explain the lack of conductivity for layers with  $[Si]_A \geq 0.5$  ML.

We speculated that  $DX$  displacements of overgrown  $Si_{Ga}$  donors takes place, thereby enhancing the rate of diffusion jumps of the Si atoms leading to the formation of Si-X and  $Si_{Ga}$ - $Si_{As}$  defects and to electrical autocompensation. Such processes should occur more readily, to yield lower values of  $n_{MAX}$  at room temperature as the growth temperature is increased. It is still unclear, however, why overcompensation occurs when  $[Si]$  is increased to too great a value for  $T_g \geq 400 \text{ }^\circ\text{C}$ . The present work has demonstrated that the limiting volume concentration  $n_{MAX}$  for the  $\delta$ -layer structures discussed here is no higher than that for homogeneously doped GaAs, and never exceeds  $\sim 2 \times 10^{19} \text{ cm}^{-3}$  in any of the samples examined.

## ACKNOWLEDGMENTS

We thank E. R. Weber (University of California at Berkeley), S. T. Pantelides (Vanderbilt University, Tennessee), P.

Hautojärvi (University of Helsinki), and C. Corbel (Saclay) for communicating their unpublished results. We similarly thank R. Jones (Exeter University) and for his many comments and discussions. J. W. thanks P. Koidl for continuous

support of the work at the Fraunhofer—Institut. The Engineering and Physical Sciences Research Council (EPSRC), United Kingdom is thanked for their financial support of the work at Imperial College (Grant No. GR/J97540).

- <sup>1</sup>K. Ploog, M. Hauser, and A. Fischer, *Appl. Phys. A* **45**, 233 (1988).
- <sup>2</sup>E. F. Schubert, *J. Vac. Sci. Technol.* **8**, 2980 (1990).
- <sup>3</sup>M. J. Ashwin, M. R. Fahy, J. J. Harris, R. C. Newman, D. A. Sansom, R. Addinall, D. S. McPhail, and V. K. M. Sharma, *J. Appl. Phys.* **73**, 633 (1993).
- <sup>4</sup>O. Brandt, G. E. Crook, K. Ploog, J. Wagner, and M. Maier, *Appl. Phys. Lett.* **59**, 2730 (1991).
- <sup>5</sup>A. Zrenner and F. Koch, in *Properties of Impurity States in Superlattice Semiconductors*, edited by C. Y. Fong, I. P. Batra, and S. Ciraci (Plenum, New York, 1988), p. 1.
- <sup>6</sup>J. J. Harris, *J. Mater. Sci.* **4**, 93 (1993).
- <sup>7</sup>J. B. Clegg and R. B. Beall, *Surf. Interf. Anal.* **14**, 308 (1989).
- <sup>8</sup>J. J. Harris, J. B. Clegg, R. B. Beall, J. Castagné, K. Woodbridge, and C. Roberts, *J. Cryst. Growth* **111**, 239 (1991).
- <sup>9</sup>J. Wagner, M. Ramsteiner, W. Stolz, M. Hauser, and K. Ploog, *Appl. Phys. Lett.* **55**, 978 (1989).
- <sup>10</sup>J. Wagner, *Proc. SPIE* **110**, 1678 (1992).
- <sup>11</sup>M. R. Fahy, M. J. Ashwin, J. J. Harris, R. C. Newman, and B. A. Joyce, *Appl. Phys. Lett.* **61**, 1805 (1992).
- <sup>12</sup>L. Hart, M. R. Fahy, R. C. Newman, and P. F. Fewster, *Appl. Phys. Lett.* **62**, 2218 (1993).
- <sup>13</sup>J. Wagner, R. C. Newman, and C. Roberts, *J. Appl. Phys.* **78**, 2431 (1995).
- <sup>14</sup>S. A. McQuaid, R. C. Newman, M. Missous, and S. O'Hagan, *J. Cryst. Growth* **127**, 515 (1993).
- <sup>15</sup>L. Hart, M. J. Ashwin, P. F. Fewster, X. Zhang, M. R. Fahy, and R. C. Newman, *Semicond. Sci. Technol.* **10**, 32 (1994).
- <sup>16</sup>R. C. Newman, in *Delta Doping of Semiconductors*, edited by E. F. Schubert (Cambridge University Press, Cambridge, 1996), pp. 279–303.
- <sup>17</sup>R. C. Newman, *Semicond. Sci. Technol.* **9**, 1749 (1994).
- <sup>18</sup>M. J. Ashwin, M. R. Fahy, L. Hart, R. C. Newman, and J. Wagner, *J. Appl. Phys.* **76**, 7627 (1994).
- <sup>19</sup>D. J. Chadi and K. J. Chang, *Phys. Rev. Lett.* **61**, 873 (1988).
- <sup>20</sup>A. R. Avery, D. M. Holmes, J. L. Sudijono, T. S. Jones, M. R. Fahy, and B. A. Joyce, *J. Cryst. Growth* **150**, 202 (1995).
- <sup>21</sup>A. R. Avery, J. L. Sudijono, D. M. Holmes, T. S. Jones, and B. A. Joyce, *Appl. Phys. Lett.* **66**, 3200 (1995).
- <sup>22</sup>M. D. Pashley and K. W. Haberern, *Phys. Rev. Lett.* **67**, 2697 (1991).
- <sup>23</sup>A. J. Dewdney, S. Holmes, H. Yu, M. R. Fahy, and R. Murray, *Superlatt. Microstruct.* **14**, 205 (1993).
- <sup>24</sup>A. B. Henriques and L. C. D. Goncalves, *Surf. Sci.* **305**, 343 (1994).
- <sup>25</sup>L. Pauling, in *The Nature of the Chemical Bond*, (Cornell University Press, Ithaca, NY, 1960).
- <sup>26</sup>R. Jones and S. Öberg, *Mater. Sci. Forum* **196-201**, 415 (1995).
- <sup>27</sup>J. E. Northrup (private communication).
- <sup>28</sup>R. C. Newman, M. J. Ashwin, J. Wagner, M. R. Fahy, L. Hart, S. N. Holmes, and C. Roberts, in *Defect and Impurity Engineered Semiconductors and Devices*, edited by S. Ashok, J. Chevallier, I. Akasaki, N. M. Johnson, and B. L. Sopori, MRS Symposia Proceedings No. 378 (Materials Research Society Pittsburgh, 1995), p. 567.
- <sup>29</sup>R. C. Newman, M. J. Ashwin, M. R. Fahy, L. Hart, S. N. Holmes, C. Roberts, and J. Wagner, *Mater. Sci. Forum* **196-201**, 425 (1995).
- <sup>30</sup>R. C. Newman, *Infrared Studies of Crystal Defects* (Taylor and Francis, London, 1973).
- <sup>31</sup>J. Wagner and M. Ramsteiner, *IEEE J. Quantum Electron.* **25**, 993 (1989).
- <sup>32</sup>M. Cardona and G. Harbeke, *J. Appl. Phys.* **34**, 813 (1962).
- <sup>33</sup>U. Fano, *Phys. Rev.* **124**, 1866 (1961).
- <sup>34</sup>M. J. Ashwin, M. R. Fahy, and R. C. Newman, *J. Appl. Phys.* **73**, 3574 (1993).
- <sup>35</sup>W. M. Theis and W. G. Spitzer, *J. Appl. Phys.* **56**, 890 (1984).
- <sup>36</sup>R. C. Newman in *Imperfections in III-V Materials*, edited by E. Weber, Semiconductors and Semimetals Vol. 38 (Academic, San Diego, 1993), pp. 117–187.
- <sup>37</sup>R. Murray, R. C. Newman, M. J. L. Sangster, R. B. Beall, J. J. Harris, P. J. Wright, J. Wagner, and M. Ramsteiner, *J. Appl. Phys.* **66**, 2589 (1989).
- <sup>38</sup>D. K. Maude, J. C. Portel, R. Murray, T. J. Foster, L. Dmowski, L. Eaves, R. C. Newman, P. Basmaji, P. Gibart, J. J. Harris, and R. B. Beall, in *Physics of DX Centers in GaAs Alloys*, edited by J. C. Bourgoin, Solid State Phenomena Vol. 10 (Sci-Tech, Liechtenstein, 1989), p. 144.
- <sup>39</sup>J. A. Wolk, M. B. Kruger, J. N. Heyman, W. Walukiewicz, R. Jeanloz, and E. E. Haller, *Phys. Rev. Lett.* **66**, 774 (1991).
- <sup>40</sup>M. Ramsteiner, J. Wagner, P. Hiesinger, and K. Köhler, *J. Appl. Phys.* **73**, 5023 (1993).
- <sup>41</sup>P. F. Fewster, *Semicond. Sci. Technol.* **8**, 1915 (1993).
- <sup>42</sup>A. G. Cullis, D. J. Robbins, A. J. Pidduck, and P. W. Smith, *J. Cryst. Growth* **123**, 333 (1992).
- <sup>43</sup>A. J. Pidduck, D. J. Robbins, A. G. Cullis, W. Y. Leong, and A. M. Pitt, *Thin Solid Films* **222**, 78 (1992).
- <sup>44</sup>A. G. Cullis, A. J. Pidduck, and M. T. Emeny, *Phys. Rev. Lett.* **75**, 2368 (1995).
- <sup>45</sup>J. Hornstra and W. J. Bartels, *J. Cryst. Growth* **44**, 513 (1978).
- <sup>46</sup>J. S. Reid, *Acta Crystallogr. A* **39**, 1 (1983).
- <sup>47</sup>J. Dobrowski and M. Scheffler, *Phys. Rev. Lett.* **60**, 2183 (1988).
- <sup>48</sup>J. D. Chadi and K. J. Chang, *Phys. Rev. Lett.* **60**, 2187 (1988).
- <sup>49</sup>H. J. Gillespie, J. K. Wade, G. E. Crook, and K. J. Matyi, *J. Appl. Phys.* **73**, 95 (1993).
- <sup>50</sup>H. Tanino, H. Kawanama, and H. Matsuhata, *Appl. Phys. Lett.* **60**, 1978 (1992).
- <sup>51</sup>E. F. Schubert, in *Doping in III-V Semiconductors*, edited by H. Ahmed, M. Pepper, and A. Broers (Cambridge University Press, Cambridge, 1993), pp. 440–443.
- <sup>52</sup>R. B. Beall, J. B. Clegg, J. Castagné, J. J. Harris, R. Murray, and R. C. Newman, *Semicond. Sci. Technol.* **4**, 1171 (1989).
- <sup>53</sup>B. Voigtländer and A. Zinner, *Surf. Sci. Lett.* **292**, L775 (1993); and (private communication).
- <sup>54</sup>T. Ohno, *Phys. Rev. Lett.* **73**, 460 (1994).
- <sup>55</sup>A. C. Warren, J. M. Woodhall, J. L. Freeouf, D. Grischowsky, D.

- T. McInturff, M. R. Melloch, and N. Otsuka, *Appl. Phys. Lett.* **57**, 1331 (1990).
- <sup>56</sup>A. C. Warren, J. M. Woodall, P. Kirchner, X. Yiu, F. Pollak, M. R. Melloch, N. Otsuka, and K. Mahalingam, *Phys. Rev. B* **46**, 4617 (1992).
- <sup>57</sup>O. Dokumaci, P. Rousseau, S. Luning, V. Krishnomoorthy, K. S. Jones, and M. E. Law, *J. Appl. Phys.* **78**, 828 (1995).
- <sup>58</sup>S. K. Pantelides (private communication).
- <sup>59</sup>H. Ono and T. Baba, *Mater. Sci. Forum* **83-87**, 1409 (1992).
- <sup>60</sup>J. Wagner, A. Fischer, W. Braun, and K. Ploog, *Phys. Rev. B* **49**, 7295 (1994).
- <sup>61</sup>H. Tanino and S. Amano, *Surf. Sci.* **267**, 422 (1992).
- <sup>62</sup>G. Brunthaler, K. Ploog, and W. Janstsch, *Phys. Rev. Lett.* **63**, 2276 (1989).
- <sup>63</sup>S. Gwo, S. Miwa, H. Ohno, J.-F. Fan, and H. Tokumoto, *Mater. Sci. Forum* **196-201**, 1949 (1995).
- <sup>64</sup>C. Corbel and P. Hautojärvi (private communication).
- <sup>65</sup>E. R. Weber (private communication).
- <sup>66</sup>J. Dabrowski and J. E. Northrup, *Phys. Rev. B* **49**, 14 286 (1994).
- <sup>67</sup>R. C. Newman, R. Jones, S. Öberg, P. R. Briddon, and M. J. Ashwin, *Solid State Commun.* **93**, 468 (1995).
- <sup>68</sup>R. Jones and S. Öberg, *Semicond. Sci. Technol.* **9**, 2291 (1994).
- <sup>69</sup>J. Maguire, R. Murray, R. C. Newman, R. B. Beall, and J. J. Harris, *Appl. Phys. Lett.* **50**, 516 (1987).
- <sup>70</sup>K. Köhler, P. Ganser, and M. Maier, *J. Cryst. Growth* **127**, 720 (1993).